

# Ray Tracing Analysis of High Frequency Communication System in Inductively Coupled Plasma Facility

Vincent Giangaspero<sup>a,b</sup>, Vatsalya Sharma<sup>a</sup>, Johannes Laur<sup>c</sup>, Jan Thoemel<sup>c</sup>, Steefan Poedts<sup>a,d</sup>, Andrea Lani<sup>a,b</sup>

<sup>a</sup>Center for Mathematical Plasma Astrophysics, KU Leuven, 3000, Belgium

<sup>b</sup>Aeronautics and Aerospace Department, Von-Karman Institute of Fluid Dynamics, 1640, Belgium

<sup>c</sup>University of Luxembourg, L-1855, Luxembourg

<sup>d</sup>Institute of Physics, University of Marie Curie-Sklodowska, ul. Radziszewskiego, Lubin, Poland

## Abstract

This work presents the numerical analysis of Radio Frequency signal propagation in an ionized plasma flow. The methodology is based on the combination of Computational Fluid Dynamics simulations and ray tracing algorithms. Different plasma flow conditions generated in the VKI plasma wind tunnel are analyzed by geometrical optics for an antenna transmitting in the Ka-band. This work is part of research efforts to improve numerical prediction and mitigation of communication blackout during atmospheric entry. An international consortium comprising universities, SMEs, research institutions, and industry has been formed to develop new technologies within the MEESST (Magnetohydrodynamic Enhanced Entry System for Space Transportation) project, which is funded by the Future and Emerging Technologies (FET) program of the European Commission's Horizon 2020 scheme (grant no. 899298).

## 1. Introduction

Atmospheric entry represents one of the most critical phases of a space mission. The safety of expensive payloads strongly depends on the spacecraft survival to the harsh conditions which are experienced during the descent into a planetary atmosphere. In this phase, a spacecraft flies at hypersonic speed, a condition characterized by the generation of high temperatures and high thermal loads on the vehicle surface. When the temperature is high enough to excite the gas molecule internal energy modes up to the point where dissociation and ionization reactions occur, a plasma layer is generated around the vehicle. Plasma interacts with the electromagnetic fields signals from/to the vehicle, disrupting the functionality of the on-board signal transmission systems [1]. The formation of entry plasma prevents radio signals to be received and transmitted from the spacecraft, leading to a communication blackout, which can last several minutes, endangering the whole mission and deeply affecting crew or payload safety. A sketch representation of this phenomenon is showed in Figure 1. The number of electrons generated in the plasma field characterizes the plasma ionization level which is quantified by the plasma natural resonant frequency in communication problems. For a given electron number density  $n_e$ , the plasma frequency can be defined as follow:

$$f_p = \frac{1}{2\pi} \sqrt{\frac{e^2 n_e}{m_e \epsilon_0}} \quad (1)$$

where  $e$  and  $m_e$  are electron charge and mass, and  $\epsilon_0$  is the free space permittivity. The created plasma layer usually has an electron number density of  $10^{17}$  to  $10^{20} \text{ m}^{-3}$  [2], depending on atmosphere composition, entry trajectory (altitude and velocity) and vehicle geometry. Plasma attenuates the radio frequency (RF) signal used for communication when the transmission frequency is comparable to the plasma frequency [3]. At each transmission frequency corresponds a plasma flow critical electron density  $n_{e,crit}$  that, if generated in the re-entry plasma layer, results in blackout conditions.

From this prospective, two different solutions are available to limit the effect of communication blackout at hypersonic speeds: the use of high frequencies transmission systems and the manipulation-reduction of plasma electron densities. In order to overcome the critical number density generated during atmospheric entry, the development and the use of high frequencies antennas are needed. However, the current technology sets a limit to transmitting antennas in the range of the Ka-band (27-40 GHz), leaving the blackout problem unsolved.

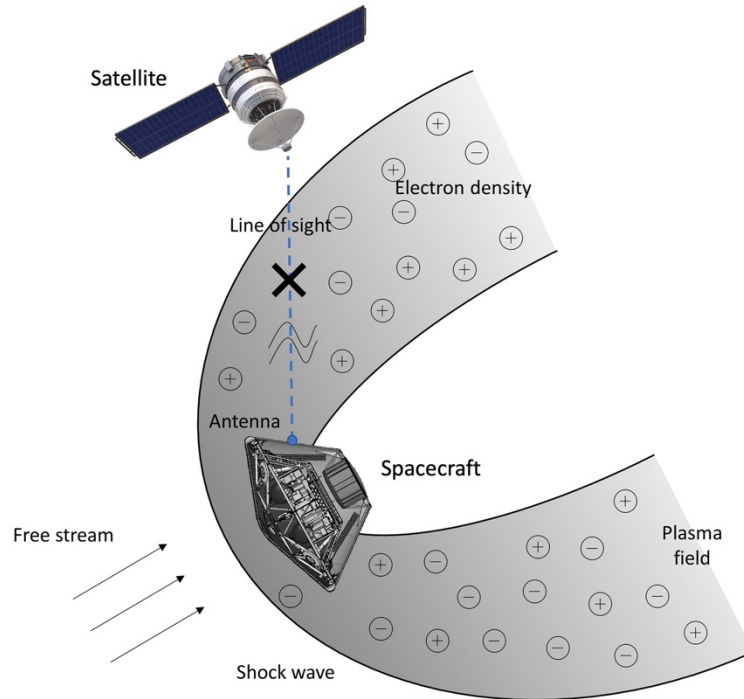


Figure 1: Radio frequency blackout for flow over entry capsule.

The current aerospace technology requires further investigations and investments to overcome this issue, especially considering the recent renewed interest in future human missions to colonize space and, in particular, Mars. As of today, spacecrafts solely rely on satellite constellations to communicate through the plasma wake, partially reducing the telecommunication blackout period, but no active system to tackle this issue has been successfully integrated into space vehicles for regular flights.

The Horizon 2020 MEESST (Magnetohydrodynamic Enhanced Entry System for Space Transportation) project aims at utilizing superconducting electromagnets to actively control the plasma surrounding a spacecraft undergoing atmospheric entry [4]. The primary aims of the project are two: to mitigate the "Radio Frequency (RF) blackout" phenomenon which disrupts all communications both to and from spacecraft during descent, and reduce the heat flux incident upon the surface of spacecraft, reducing the need for heavy thermal protection systems (TPS). Both goals are to be achieved by taking advantage of magnetohydrodynamic (MHD) effects, i.e. using electromagnetic fields to manipulate the charged plasma sheath surrounding a spacecraft. The RF blackout phenomenon may be mitigated by creating a region of plasma with a volumetric electron density low enough for RF transmissions to leave the plasma without being deflected or absorbed. MEESST includes experimental campaigns in the plasma wind tunnels of the Von Karman Institute (VKI) and the Institute of Space System (IRS), and numerical simulations relying upon improved models.

As a part of this project, this work presents a numerical methodology to analyse the interaction between high frequency radio signals and an ionised plasma flow. The interaction between the electromagnetic waves and the ionised plasma will be analysed by the application of an optical ray tracing method. The use of an advanced blackout analysis method capable of reproducing more complex waves phenomena, such as reflection, refraction and phase modulation, has the advantage of improving the overall understanding of the complex physical phenomena involved in the blackout problem. The use of ray tracing methods for analysing communication entry problems has already proved his potential. Two-dimensional ray tracing analysis were performed for the ExoMars Schiaparelli re-entry capsule [5,6] and for the Atmospheric Re-entry Demonstrator (ARD) [7]. In this work, this methodology is applied to the two-dimensional analysis of the air plasma flow produced with the Inductively Coupled Plasma (ICP) generator in the VKI-Plasmatron facility. The ray tracing analysis will be used to assist the experimental campaign design, focusing on the signal pattern inside the facility with respect to different antenna transmission frequencies, antenna location and plasma conditions. The numerical analysis conclusions will be validated with the ongoing experimental campaign, of which preliminary results are reported by Luis et al. [8].

## 2 Methodology : BORAT-BlackOut RAY Tracer

Numerical analysis of communication blackout involves two different steps: first the calculation of electron density profiles from Computational Fluid Dynamics (CFD) simulations; second the modeling of the RF signal propagation through plasma. Due to the different time scales of these phenomena, the plasma variation in time can be considered slow with respect to the RF signal propagation. This allows for analysing re-entry communication blackout by simulating different flow field conditions, in which plasma is considered constant while solving the wave propagation in its interior. To analyze the propagation of electromagnetic (EM) waves in plasma, the modeling strategies are generally divided in full wave methods and ray tracing methods. Full wave methods, i.e. FDTD. and FEM , solve the full set of Maxwell equations without approximation, with the drawbacks of different time steps required by the EM and fluid phenomena, leading to larger computational costs. This makes their use particularly disadvantageous for large propagation problems, such as in space entry applications. For this reason, the use of ray tracing methods is particularly indicated to analyze large propagation problems, since they are based on approximate solutions of Maxwell equations, reducing the complexity of the numerical simulation. Ray tracing method results in numerically efficient solvers, in which EM waves wavefronts are discretized with a beam of ray: each ray is independent and uncoupled with respect to the other rays, allowing for an easy parallelization, with a complexity that scales linearly.

The application of ray tracing techniques to space re-entry communication has been proved to be a valid and promising approach to describe the phenomena involving communications blackout [5,6]. The ray tracing technique employed in this work has been implemented in the the BlackOut Ray Tracer solver (BORAT). More details on the implementation of the ray tracing methodology will be discussed in the following sections.

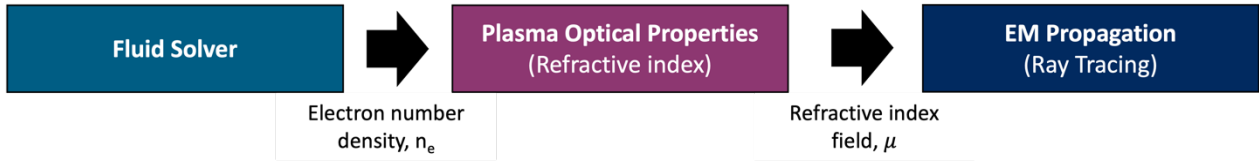


Figure 2: Illustration of the numerical analysis methodology for ray tracing method.

### 2.2 Optical plasma model

The first step for the application of ray tracing is the computation of optical properties of plasma governing the propagation of EM waves in a medium. The flow field solution obtained from the CFD simulations contain the information needed to construct the numerical model of the plasma. The optical properties are described by the Appleton-Hartree equation, that calculates the refractive index for electromagnetic wave propagation in a cold unmagnetized plasma. In the context of this project, the fundamental theory behind optical properties follows the description of Davies [9], who derives the Appleton equation based on the Maxwell equations and the conservation of momentum of free electrons. It reads as:

$$n^2 = (\mu - \chi i)^2. \quad (2)$$

In this formulation, the plasma is characterized by the complex refractive index  $n$ , consisting of a real part,  $\mu$ , and an imaginary part,  $\chi$ . The real part  $\mu$  represents the effect of plasma in waves propagation bending, while the imaginary part  $\chi$  represents the absorptivity, responsible of attenuation effects on travelling waves. The full equation form reads as follows:

$$n^2 = (\mu - \chi i)^2 = 1 - \frac{X}{1 - Zi}, \quad (3)$$

with

$$\begin{aligned} X &= e^2 n_e / (\epsilon_0 m_e \omega^2) \\ Z &= v / \omega \\ \omega &= 2\pi f, \end{aligned} \quad (4)$$

where  $e$  denotes the electron charge,  $n_e$  the electron number density,  $\epsilon_0$  the vacuum permittivity,  $m_e$  the electron mass,  $\nu$  the electron-heavy particle collision frequency,  $f$  for the communication system transmission frequency. For this work, the reduced form of the Appleton-Hartree equation for unmagnetized cold plasma is used, in which the effect of magnetic fields is neglected in the computation of the refractive index. This is the general case of atmospheric re-entry plasma, in which no magnetic fields are applied on the spacecraft and planetary magnetic fields can be neglected. Future work will take into account the effect of MHD active devices on the computation of the refractive index. Solving equation 2 for  $\mu$  and  $\chi$  leads to:

$$\mu^2 = \frac{1}{2} \left( 1 - \frac{X}{1+Z^2} \right) + \frac{1}{2} \sqrt{1 - 2 \frac{X}{1+Z^2} + \frac{X^2}{1+Z^2}} \quad (5)$$

$$\chi^2 = -\frac{1}{2} \left( 1 - \frac{X}{1+Z^2} \right) + \frac{1}{2} \sqrt{1 - 2 \frac{X}{1+Z^2} + \frac{X^2}{1+Z^2}}. \quad (6)$$

The resulting equation becomes a function of  $X$ , which is a direct function of the electron number density  $n_e$ , and  $Z$ , which is a direct function of the collision frequency  $\nu$ . Figure 3 shows the effect of the collision frequency on the real part of the refractive index,  $\mu$ , that governs ray's path bending in ray tracing theory. Taking into account the collisional frequency between electrons and heavy particles, equation (2) yields to a complex refractive index  $n$ , with non-zero values of the absorptivity coefficient. In this case collisions affect the absorption of the transmitted signal, but they have also an effect on the real part of the refractive index. The line  $Z=0$  represent a non-collisional medium, in which increasing the  $X$  value (thus increasing the ratio between electron number densities and transmission frequency), decreases the refractive index  $\mu$ . By increasing the value of  $Z$  we see a deviation from the linear refractive index trend and for high values of collision frequency, the refractive index doesn't reach zero values, but attains a minimum value. In these conditions total reflection never really occurs.

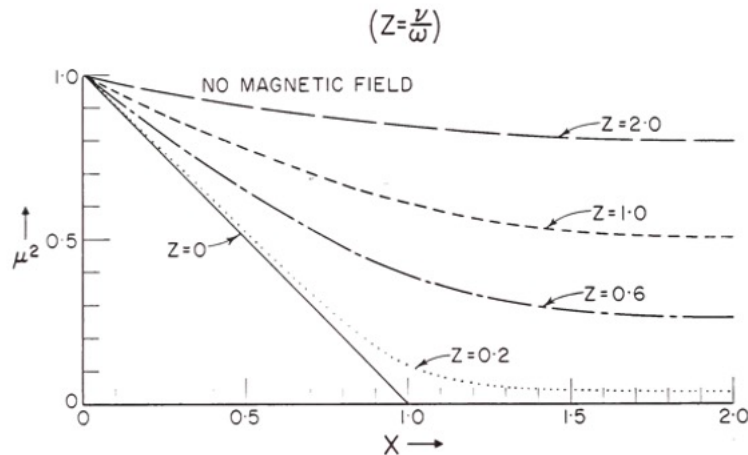


Figure 3: Deviation of refractive index  $\mu$  with  $X$  for different collisional frequencies [9].

The effect of collision frequency is expressed by the absorptivity coefficient, that represents the exponential decreasing amplitude of a one-dimensional traveling wave [9] and the following quantity:

$$k = \frac{2\pi f}{c} \chi. \quad (6)$$

is a measure of the decay of amplitude per unit distance and is called absorption coefficient  $k$ . This formula gives the absorption in nepers per meter, where 1 neper=8.69 dB. By integrating the absorption coefficient along the path of the transmitted signal, it is possible to calculate the total attenuation due to absorption by collision with charged particles.

### 2.3 Ray tracing algorithm: Eikonal theory

Ray tracing theory is founded on geometrical optics, and provides a reliable method to estimate the dominant path of energy flow in propagating EM waves. The algorithm implemented in the BORAT solver belongs to the family *shooting and bouncing* ray tracing (SBR) technique [11], in which rays are emitted from the antenna location and integrated in the numerical domain until they emerge from the plasma. The optical properties of plasma computed by the application of the Appleton-Hartree equation define the numerical domain of the ray tracing integration, and are used as a starting point for the ray tracing analysis. The ray integration technique used in this work is an advanced ray tracing method based on the Eikonal equation. The Eikonal equation can be derived as an approximate solution of Maxwell's equations in the high-frequency range limit [12]. It reads as:

$$|\nabla S| = \mu, \quad (7)$$

where  $S$  is the normalised Eikonal phase function, defining the wave-front surface of a traveling electromagnetic wave, and  $\mu$  is the real part of the refractive index of the medium. The equation (7) can be rewritten in characteristic form, with the advantage of a more convenient representation to retrieve ray trajectories equations. This may be achieved by introducing the normalized local wave vector  $\xi_i = \nabla S$ , that defines the propagation direction of the EM wave, and the position vector  $x_i$ . Using the arc-length  $s$  along the ray, one arrives at the following system of ordinary differential equations:

$$\frac{\partial x_i}{\partial s} = \frac{\xi_i}{\mu} \quad (8)$$

$$\frac{\partial \xi_i}{\partial s} = \frac{\partial \mu}{\partial x_i} \quad (9)$$

The characteristic solution of the Eikonal equation defines the rays trajectories. The system (8-9), along with prescribed initial conditions in terms of position and angle of the emitted ray, allows for predicting ray trajectories and states that the curvature of rays at each point is proportional to the gradient of the refractive index.

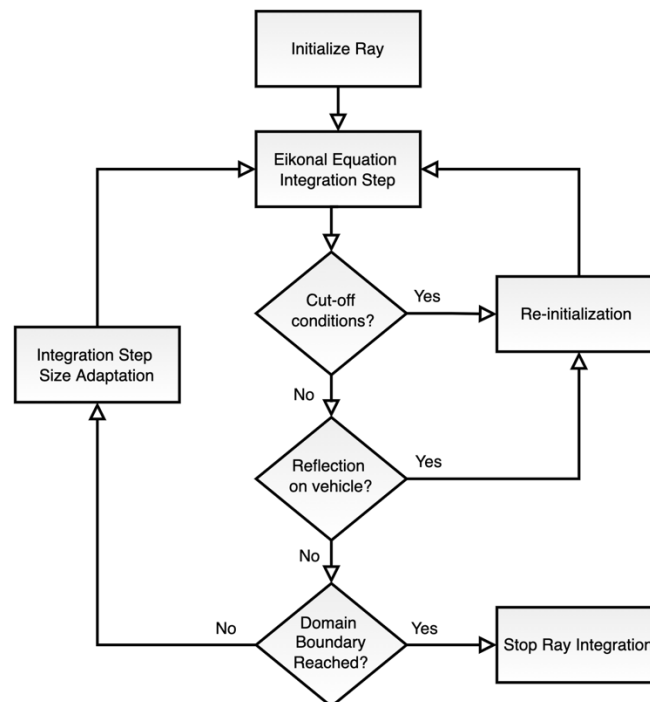


Figure 4: Ray tracing algorithm

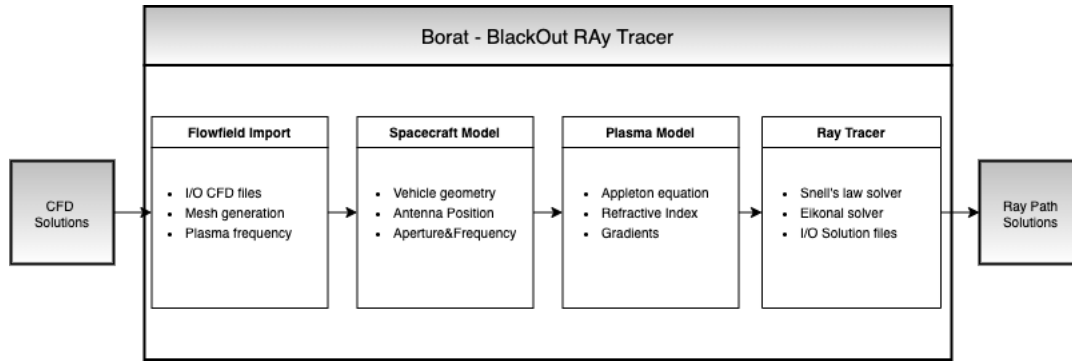


Figure 5: Flowchart of the BORAT ray tracing code

The Eikonal ray trajectories are implemented in the BORAT ray tracing solver, a MATLAB software developed by the University of Luxembourg and KUL to analyse space re-entry blackout problems. Figure 5 shows a flowchart of the BORAT code and its main constitutive parts. To summarize, the numerical strategy for the communication blackout ray tracing analysis is composed by:

- CFD simulations of ionised plasma flows at different conditions;
- computation of optical properties of plasma by the application of the Appleton-Hartree equation for the specific plasma model;
- application of ray tracing to propagate the EM waves through plasma.

### 3. Results and discussion

In this section the results of the ray tracing analysis of high frequency signal propagation in an Inductively Coupled Plasma (ICP) facility will be presented. The goal of study is to contribute with a numerical analysis to design the experimental campaign on communication blackout that will be conducted as part of the MEESST project. VKI is the consortium's leading partner for experimental studies related to MEESST, especially for topics concerning radio blackout mitigation. The VKI offers plasma facilities with ICP generators delivering powers up to 1.2 MW, capable of operating with air or CO<sub>2</sub>, enabling the reproduction of entry conditions similar in composition to Earth's or Martian atmospheres [13]. The Plasmatron facility at VKI, which will be used for the radio communication blackout experiments in MEESST, is shown in Figure 6. More information on the facility and the experimental campaign can be found in [8].

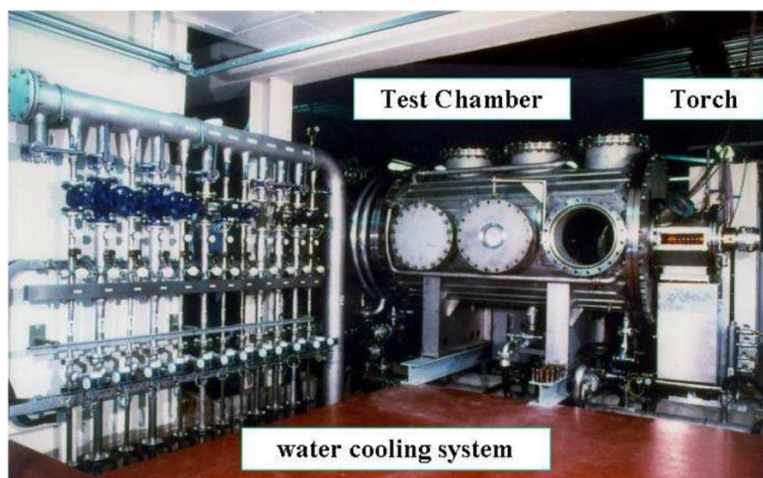


Figure 6: The VKI-Plasmatron facility

### 3.1 CFD simulations

The numerical analysis starts with simulations of the plasma flow in the Plasmatron experimental facility. A schematic of the chamber set-up is represented in Figure 7. For this purpose, a database of numerical simulations [14] has been used to perform a preliminary study on the optical properties of the plasma flow generated in the facility.

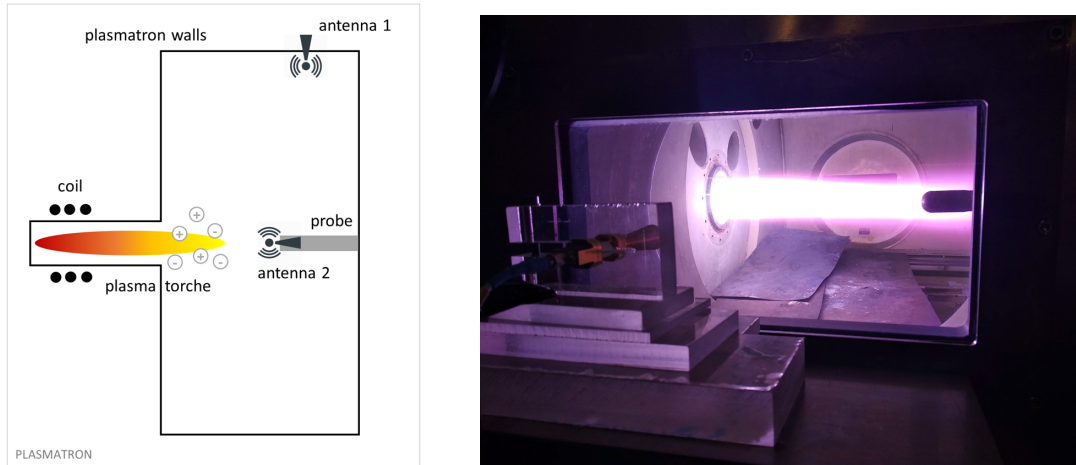


Figure 7: Scheme of the experimental set-up (left) and photo taken during a test (right) [8].

The subsonic steady state plasma flow field in the Plasmatron chamber is numerically simulated using an inhouse-developed ICP model [15] which couples the Maxwell equations with the Navier-Stokes equations under Local Thermodynamic Equilibrium (LTE), assuming axisymmetric steady flows and which is implemented into the Computational Object-Oriented Library for Fluid Dynamics COOLFluid [16]. This solver simulates the interaction between the electromagnetic field around the coil and the gas passing through, with the aim of reproducing the whole Plasmatron chamber. The ICP computations use the VKI developed Mutation++ [17] library to determine thermodynamic and transport properties of the 11-species air mixture, including  $O_2$ ,  $N_2$ ,  $O^{+2}$ ,  $N^{+2}$ ,  $NO$ ,  $NO^+$ ,  $O$ ,  $O^+$ ,  $N^+$ ,  $N$  and  $e^-$ . In the simulations, all the walls are cooled down to 350 K and the annular injection of the gas is imposed at the inlet [14].

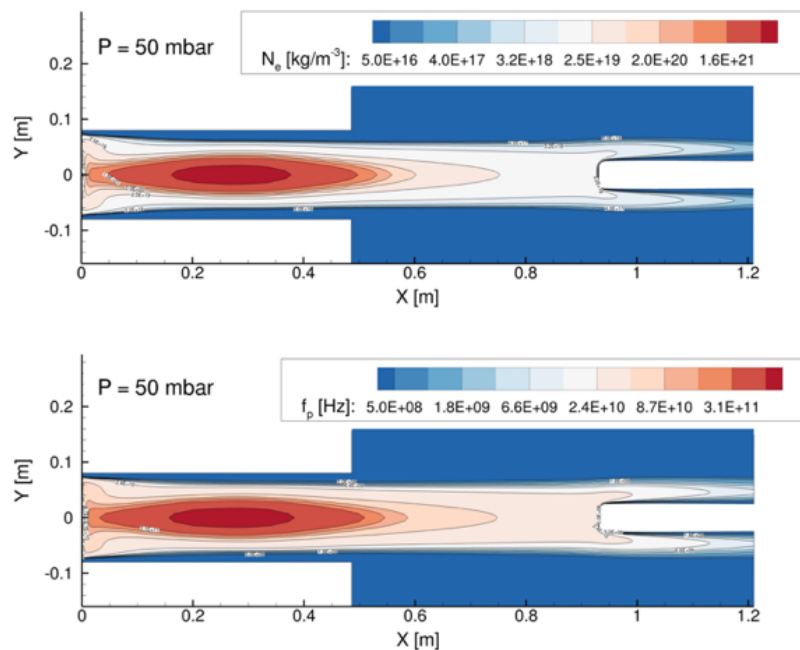


Figure 8: Electron number density field (top) and plasma frequency (bottom) for test simulation at 50 mbar, 71 kW of power and 16 g/s of mass flow.



The input parameters for the numerical simulations of the ICP generated plasma flow are the static pressure in the Plasmatron chamber, the gas mass flow rate supplied to the torch, and the effective power dissipated in the plasma by electromagnetic induction. The exact value for the effective power generating the plasma in the facility is unknown and generally an efficiency of 50% of the electric power is considered [8]. For this reason, the nominal power torch values considered in this numerical analysis are considered 50% lower respect the effective power used in the experimental conditions.

### 3.2 Optical properties of the plasma flow

The first tests have been conducted to analyze the effect of two different factors: pressure condition in the chamber and transmitting antenna frequency. The objective is to identify the most favorable and effective conditions for the experiments design. The following analysis considers a database of simulations at a constant mass flux of 16 g/s, static pressures of 15 and 50 mbar, and varied effective powers, under LTE assumption. The optical properties of the flow are computed in the Ka-band, between 27 and 40 GHz. The flow field generated in the facility is shown in Figure 8, in terms of electron number density and plasma frequency, for chamber pressure 50 mbar and 71 kW torch power.

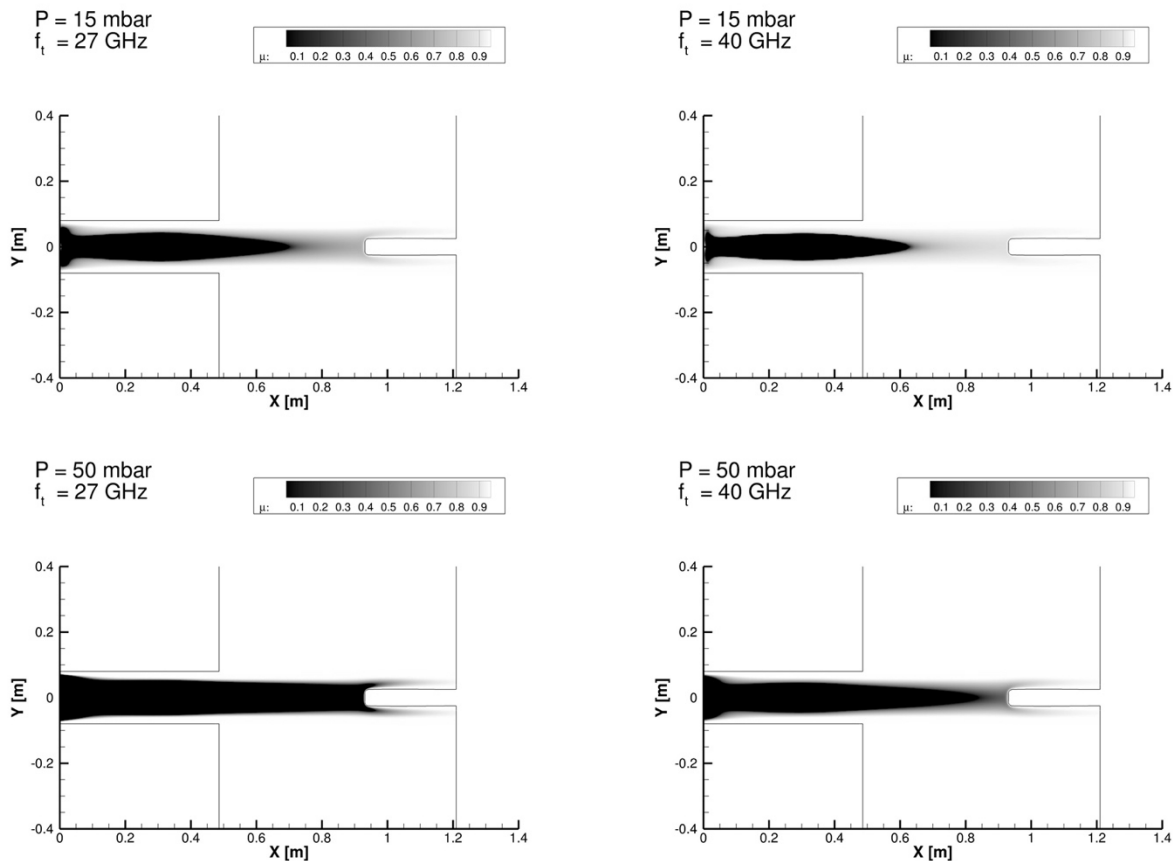


Figure 9: refractive index fields at different chamber pressure conditions (15-50 mbar) and transmission frequency (27-40 GHz).

Figure 9 shows the calculation of the optical properties of the flow for each combination of plasma conditions and transmission frequency. The calculation of the plasma absorption shows how high values of collisional frequency (and thus signal attenuation by absorption) are confined to the torch zone, as seen in Figure 10. This important result confirms the hypothesis that the signal will not be absorbed in the facility, but reflected and refracted by the plasma. The refractive index field show how the most favorable conditions for communication through the plasma belong to lower chamber pressure conditions, in which ionization levels on the stagnation line are lower. As expected, with the increase of the communication system frequency, the plasma shielding effect decreases, allowing a deeper penetration



of the RF signal in the plasma. Following the computation of optical properties of the flow, the next step has been the ray tracing analysis of the emitted signal and its interaction with the plasma flow, that will be described in the next section

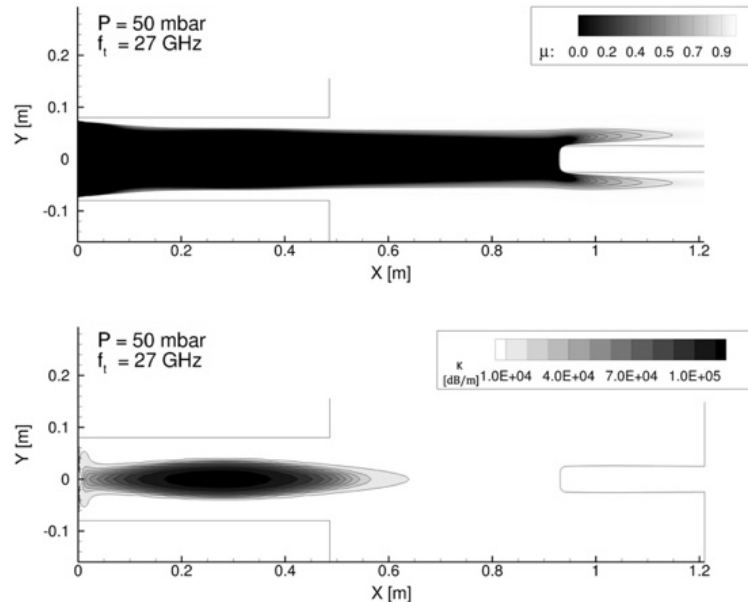


Figure 10: Refractive index (top) and collisional absorption (bottom) for test simulation at 50 mbar, 71 kW of power and 16 g/s of mass flow, for a transmission frequency of 27 GHz.

### 3.3 Ray Tracing analysis

For the ray tracing analysis, two different experimental designs have been considered, characterized by a different transmitting antenna location. The first configuration is the side-to-side communication, in which the antenna is located on one side of the facility metallic chamber, with the purpose of communicating through the plasma layer and reach a receiver located on the other side of the chamber. The results of this analysis are showed in Figure 11. The interest in the side-to-side experimental set up is the simplicity in placing and protecting the emitting antenna and receiving devices in the facility, since temperature peaks far from the stagnation line are lower.

Results show how ionization levels at lower pressure chamber (15 mbar) allow penetration of RF signal through the plasma flow. At lower transmission frequency (27 GHz), signal is partially reflected by the plasma, while at higher frequency (40 GHz) signal is slightly refracted. At higher pressure chamber (50 mbar) the highly ionized flow extends along the whole stagnation line, reaching the probe tip. In these conditions the transmission frequency is irrelevant, since the highly ionized flow will always reflect the transmitted signal.

Figure 12 shows the result of the front communication set up. In this case, the emitting antenna is placed inside the probe and will emit the signal towards the front part of the Plasmatron chamber, emulating a similar configuration as that proposed with the presence of a magnet in the framework of MEESST. For this configuration, the ray tracing analysis shows that communication is favorable only at lower values the chamber pressure (15 mbar). In these conditions the angular deviation of the emitted signal is directly related to the ionization level of the flow, and this will be one of the parameters that will be used in future for the validation of the ray tracing analysis with the actual experiments. At fixed flow conditions, increasing the transmission frequency (27 to 40 GHz) decreases the deviation angle, with a behaviour that is inversely proportional to transmission frequency. Higher chamber pressures (50 mbar) generate high values of ionization on the stagnation line that completely prevent communication at lower frequencies, and signal escapes the plasma layer only at higher frequency. For these conditions, the front communication set up is not recommended. The conclusions of the first analysis indicates that low operating pressure in the facility generates lower level of ionization in the plasma. The advantage is that for low pressures and for transmission frequencies in the range of 27 to 40 GHz allow for different experiment designs, increasing the feasibility of the whole experimental campaign.

The second round of analysis has been focused on the effect of the plasma torch power on the RF signal and plasma interaction. For this study chamber pressure conditions (15 mbar) and transmission frequency (38.5 GHz) have been kept fixed, with the intent of finding the most valuable operating range of torch powers for the experiment design. Results are shown in Figure 12, in which the torch power varies between 56 and 102 kW.

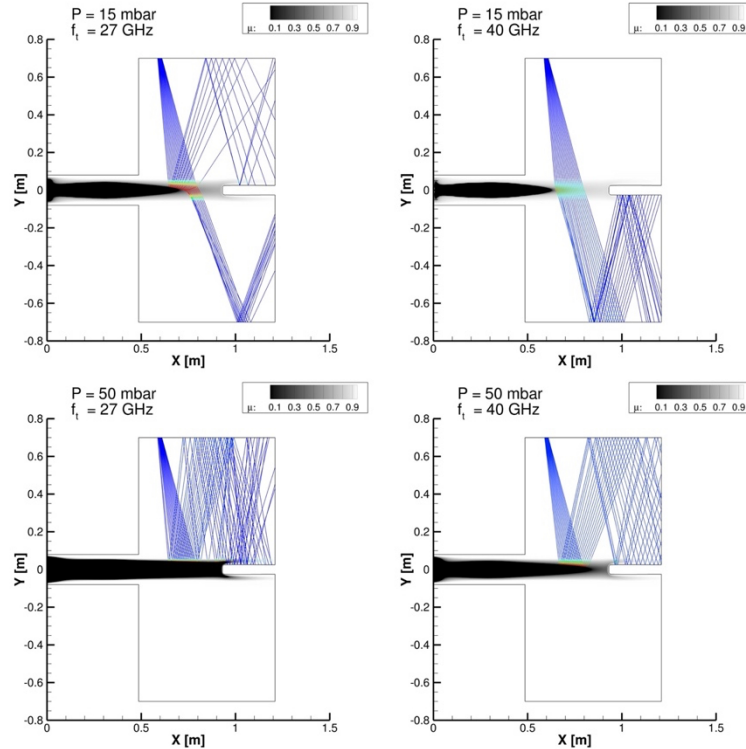


Figure 11: 2D Ray tracing analysis of side-to-side experimental set-up (antenna on chamber's wall) for different pressure chambers and antenna transmission frequency

The conclusions of the second analysis are that the maximum torch power allowed for communication in these conditions (fixed pressure and transmission frequency) are around 100 kW, value above which RF signal will not escape the plasma surrounding the probe. Increasing the torch power will change the deviation of the emitted signal with respect to the symmetry axis, allowing to calibrate the experiments conditions to the most suitable design.

#### 4. Conclusions and future work

This work presents the numerical analysis of radio signal propagation within the air plasma flow generated in the VKI ICP Plasmatron facility. This study was conducted to assist the design of the experimental campaign on communication blackout foreseen at VKI within the MEESST project. The methodology is based on the combination of CFD simulations and optical ray tracing method. Different combinations of plasma flow have been analysed, based on ICP simulations of the Plasmatron facility in LTE conditions, characterized by different static pressure and torch power. The transmission frequency analyzed in this work belongs to the Ka-band between 27 and 40 GHz. Two different antenna locations have been considered to analyze the interaction between the RF signal and the plasma flow. The preliminary investigation led to the conclusion that the plasma flow generated in such conditions interacts with emitted RF signal by reflection and refraction, but not absorption. The effect of different flow conditions has been analyzed and the most favorable conditions for the experimental campaign have been identified. These preliminary results show how the ray tracing is a suitable tool to provide useful information to assist the design of the experimental campaign of the MEESST project. Future work will be focused on the validation of these results with the data produced in the experimental campaign.

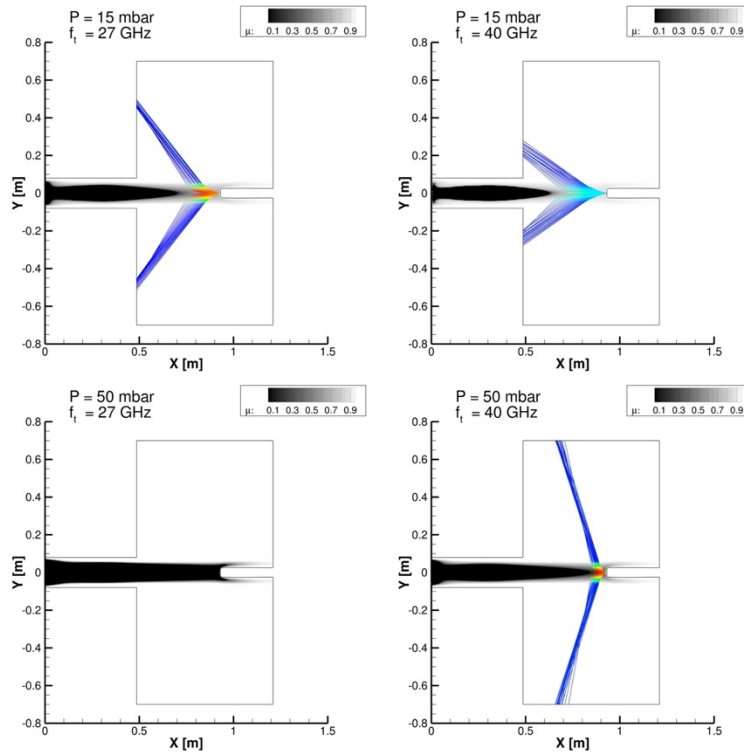


Figure 11: 2D Ray tracing analysis of front experimental set-up (antenna inside the probe) for different pressure chambers and antenna transmission frequency.

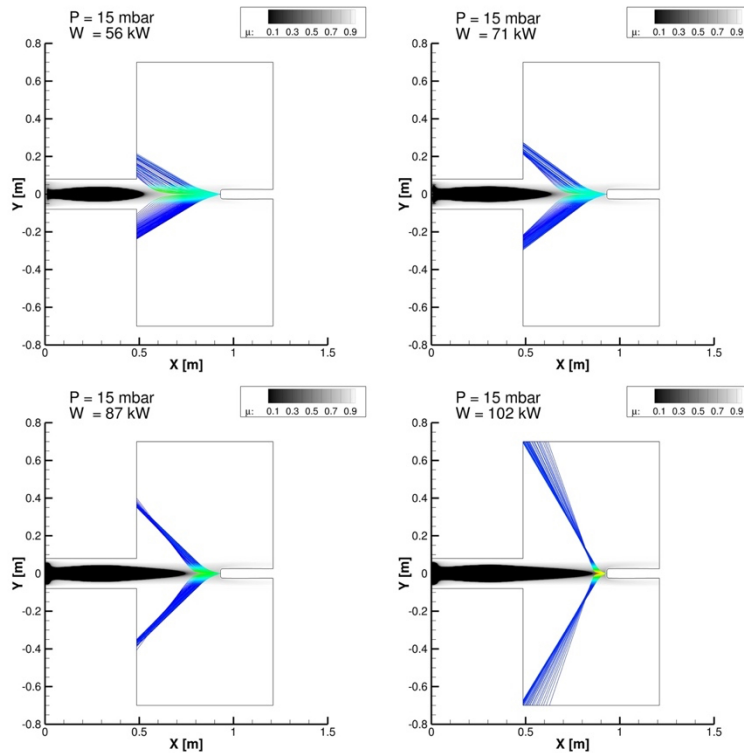


Figure 12: 2D Ray tracing analysis of front experimental set-up for different torch powers, at fixed pressure (15 mbar) and fixed antenna transmission frequency (38.5 GHz).

## 5. Acknowledgements

This project has received funding from the European Union's Horizon 2020 Research and Innovation Program under grant agreement 899298. This paper reflects only the authors' view, and the European Commission is not responsible for any use that may be made of the information it contains. The research of Vincent Fitzgerald Giangaspero is supported by SB PhD fellowship 1SA8219N of the the Research Foundation - Flanders (FWO). The resources and services used in this work were provided by the VSC (Flemish Supercomputer Center), funded by the Research Foundation - Flanders (FWO) and the Flemish Government.

## References

- [1] Kim, M. (2014). Active plasma layer manipulation scheme during hypersonic flight. *Aerospace Science and Technology*, 35, 135-142.
- [2] Boyd, I. (2007, January). Modeling of plasma formation in rarefied hypersonic entry flows. In *45th AIAA Aerospace Sciences Meeting and Exhibit* (p. 206).
- [3] Morabito, D., Kornfeld, R., Bruvold, K., Craig, L., & Edquist, K. (2009). The mars phoenix communications brownout during entry into the martian atmosphere. *The Interplanetary Network Progress Report*, 42, 179.
- [4] Bögel, E., La Rosa Betancourt, M. A., & Collier-Wright, M. R. (2021). Magnetohydrodynamic Enhanced Entry System for Space Transportation (MEESST) as a Key Building Block for Future Exploration Missions. In *AIAA Propulsion and Energy 2021 Forum* (p. 3272).
- [5] Ramjatan, S., Lani, A., Boccelli, S., Van Hove, B., Karatekin, Ö., Magin, T., & Thoemel, J. (2020). Blackout analysis of Mars entry missions. *Journal of Fluid Mechanics*, 904.
- [6] Giangaspero 2021 Giangaspero, V. F., Lani, A., Poedts, S., Thoemel, J., & Munafò, A. (2021). Radio communication blackout analysis of ExoMars re-entry mission using raytracing method. In *AIAA Scitech 2021 Forum* (p. 0154).
- [7] Vecchi, C., Sabbadini, M., Maggiora, R., & Siciliano, A. (2004, June). Modelling of antenna radiation pattern of a re-entry vehicle in presence of plasma. In *IEEE Antennas and Propagation Society Symposium, 2004.* (Vol. 1, pp. 181-184). IEEE.
- [8] Luis, D., Viladegut A., Camps, A., Chazot, O., (2022) Effect of electron number densities on the radio signal attenuation in an inductively coupled plasma facility. In: EUCASS 2022 Conference Paper
- [9] Davies Davies, K. (1965). *Ionospheric radio propagation* (Vol. 80). US Department of Commerce, National Bureau of Standards.
- [10] Yunxian Tian, Weizhong Yan, Xiaoliang Gu, Xiaolin Jin, Jianqing Li, and Bin Li, "Effects of magnetized plasma on the propagation properties of obliquely incident THz waves," AIP Advances, vol. 7, no. 12, pp. 125325, dec 2017.
- [11] Ling, H., Chou, R. C., & Lee, S. W. (1989). Shooting and bouncing rays: Calculating the RCS of an arbitrarily shaped cavity. *IEEE Transactions on Antennas and propagation*, 37(2), 194-205.
- [12] Kravtsov, Y. A., & Orlov, Y. I. (1990). *Geometrical optics of inhomogeneous media* (Vol. 38, p. 48). Berlin: Springer-Verlag.
- [13] Bottin, B., Chazot, O., Carbonaro, M., Van Der Haegen, V., & Paris, S. (2000). *The VKI plasmatron characteristics and performance*. VON KARMAN INST FOR FLUID DYNAMICS RHODE-SAINT-GENESE (BELGIUM).
- [14] A. Viladegut. 2017. *Assessment of gas-surface interaction modelling for lifting body re-entry flight design* (Doctoral dissertation, Universitat Politècnica de Catalunya (UPC)).
- [15] G. Degrez, G., Abeele, D. V., Barbante, P., & Bottin, B. (2004). Numerical simulation of inductively coupled plasma flows under chemical non-equilibrium. *International Journal of Numerical Methods for Heat & Fluid Flow*.
- [16] Lani, A. (2008). An object oriented and high performance platform for aerothermodynamics simulation. *Université Libre de Bruxelles*.
- [17] Scoggins, J. B. (2017). *Development of numerical methods and study of coupled flow, radiation, and ablation phenomena for atmospheric entry* (Doctoral dissertation, von Karman Institute for Fluid Dynamics).